PHYSICAL REVIEW B VOLUME 25, NUMBER 6 15 MARCH 1982

Pressure dependence of the optical phonons and transverse effective charge in 3C-SiC

Diego Olego and M. Cardona
Max-Planck Institut für Festkörperforschung, 7000 Stuttgart 80, Federal Republic of Germany

P. Vogl
Institut für Theoretische Physik, Universität Graz, 8010 Graz, Austria

(Received 28 August 1981)

The first-order Raman spectra of 3C-SiC have been measured as a function of hydrostatic pressure up to 22.5 GPa in a diamond anvil cell. The mode-Grüneisen parameters of the LO and TO phonons at Γ were determined. We observed an *increase* of the LO-TO splitting with pressure from which an *increase* of the transverse effective charge upon compression results. We discuss this behavior of the transverse effective charge under lattice compression in terms of a microscopic pseudopotential calculation and of the bond-orbital model. Calculations of effective charges for other hypothetical IV-IV semiconductors are presented.

I. INTRODUCTION

Useful information about the vibronic properties, structural phase transitions, and covalency of semiconductors can be obtained by measuring the dependence of the phonon spectrum on high hydrostatic pressure. Such experiments also provide very stringent tests for lattice-dynamical theories. The development of the diamond anvil cell in conjunction with the ruby fluorescence manometer has given new impetus to the spectroscopic investigations of the vibronic and electronic properties of semiconductors under high pressure.[1] The diamond anvil cell is particularly suited to perform light scattering, as well as absorption and luminescence measurements.[2–5] With it the pressure dependence of phonon frequencies can be studied by means of first- and second-order Raman scattering.

The behavior of the phonon spectra under hydrostatic pressure has been reported for the elemental semiconductors of the group IV,[2,6] as well as for III-V,[2,4,7] II-VI,[8] and I-III-VI,[9] compounds. Most of these investigations have been performed for pressures up to the phase transitions.[10] We report in this paper the dependence of the long-wavelength ($\vec{q}\simeq 0$) optical phonons of cubic (3C-type) SiC on hydrostatic pressure. This modification of SiC crystallizes in the zinc-blende structure so that three optical modes are present at the Γ point. Owing to the difference in the electronegativity of Si and C the three optical modes at Γ are split into two degenerate transverse optical modes [TO(Γ) modes] and a nondegenerate longitudinal optical mode [LO(Γ) mode]. We report here the dependence on pressure of the frequencies of the TO(Γ) and LO(Γ) modes of 3C-SiC measured for pressures up to 22.5 Gpa using first-order Raman scattering. The second-order Raman spectrum of 3C-SiC as a function of pressure will be the subject of another publication.

The motivation of the present work is twofold: to contribute to the systematic study of the effects of pressure on the phonons of the zinc-blende-type semiconductors and to investigate carefully the effect of pressure on the Born's transverse effective charge e_T^* (the dynamical charge) for 3C-SiC, a zinc-blende-type semiconductor with an ionicity of a type different from that encountered in the III-V and II-VI compounds. The LO(Γ)-TO(Γ) splitting has been found to become smaller as a function of pressure in the III-V (Refs. 2, 4, and 7) and II-VI (Ref. 8) compounds. Correspondingly, the dynamical charge obtained from the splitting decreases with increasing pressure, which means that the semiconductor material becomes more covalent upon compression. Microscopic theoretical calculations of e_T^* as well as a semiempirical bond-orbital model reproduce this measured behavior of the dynamical charge.[4,11,12]

This increase in covalency with increasing pressure characteristic of the III-V and II-VI semiconductors was definitely established after measurements to very high pressure became possible with

the diamond anvil cell. In an early work (pressures lower than 1 GPa) Mitra *et al.*[13] reported an *increase* in the LO(Γ)-TO(Γ) splitting of GaP and 3*C*-SiC. In the case of GaP it was proved later by the measurements of Weinstein and Piermarini[2] (pressures up to 13.5 GPa) that the low-pressure results of Mitra *et al.*[13] were incorrect. This LO(Γ)-TO(Γ) splitting of GaP behaves as those of GaAs,[7] InP,[4] and the II-VI compounds.[8] The sign of the pressure coefficient of the LO-TO splitting in SiC thus remained an open question.

We report here the observation of an *increase* of the LO(Γ)-TO(Γ) splitting of 3*C*-SiC with increasing pressure up to 22.5 GPa, which corresponds to an increase of e_T^* upon compression. Thus 3*C*-SiC becomes more *ionic* as a function of pressure, opposite to the more common systematic behavior of other zinc-blende semiconductors.

The increase in e_T^* observed for 3*C*-SiC with increasing pressure can be accounted for by microscopic calculations based on an empirical pseudopotential.[11] The semiempirical bond-orbital model, however, is unable to account for these results. We also present, as a by-product, results of calculations of e_T^* and the polarity α_p for other IV-IV (e.g., Si-C) hypothetical semiconductors.

II. EXPERIMENTAL DETAILS

The 3*C*-SiC samples used for the high-pressure work were cut from single crystals grown at Westinghouse Research Laboratories and kindly given to us by Dr. W. J. Choyke. For the pressure measurements the 3*C*-SiC samples, which were light yellow, were broken into small pieces and one of them, suitable to fit into the 200-μm hole of the pressure-cell gasket, was chosen under the microscope.

A gasketed diamond anvil cell, such as the one described by Syassen and Holzapfel,[14] was employed for the Raman measurements. A 4:1 methanol-ethanol mixture served as the pressure medium and the fluorescence of a small ruby chip placed near the 3*C*-SiC sample was used for pressure calibration.[1]

The backscattering geometry was adopted to perform the experiment.[2] The Raman spectra were excited with the 5145-Å (2.41 eV) line of an Ar^+-ion gas laser. The scattered light was analyzed with a Spex 1402 double monochromator, equipped with holographic gratings, and detected with a cooled RCA C31034 photomultiplier by means of photon counting. All measurements were carried out at room temperature.

III. RESULTS AND DISCUSSION

Figure 1 displays typical first-order Stokes Raman spectra of the TO and LO phonons of 3*C*-SiC for various pressures at room temperature. With increasing hydrostatic pressure the LO and TO Raman lines shift to higher energies. We measured these shifts for pressures up to 22.5 GPa; the upper limit in the value of the pressure was determined by the type of diamond anvil cell used. Up to 22.5 GPa we did not observe any indication of a possible phase transition. The photon energy of the laser line used to excite the spectra (2.41 eV) lies near the fundamental absorption edge of 3*C*-SiC.[15] Hence the Raman measurements were performed under near-resonant conditions. This fact allowed us to obtain strong Raman signals even at very low pressures. Therefore it was not necessary to measure the phonon lines for zero pressure with the sample *outside* the diamond anvil cell, as was the case in experiments carried out with materials opaque to the exciting laser lines.[7] The frequencies of the TO and LO modes for zero pressure agree within the experimental error with the values reported by other authors.[13,16] The wave number scales in Fig. 1 are drawn in such a way to display the fact that the LO(Γ)-TO(Γ) splitting increases with increasing pressure.

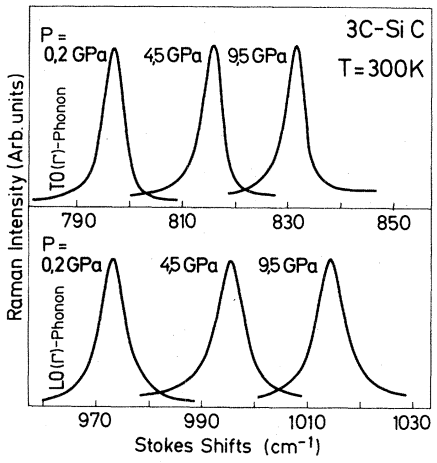

FIG. 1. First-order Raman spectra of 3*C*-SiC obtained at room temperature under different hydrostatic pressures. The wave number scales are drawn in such a way as to display the increase of the LO(Γ)-TO(Γ) splitting with increasing pressure.

Figure 2 shows the peak positions of the LO and TO Raman lines as a function of the pressure (top horizontal scale) and of the relative lattice compression $-\Delta a/a_0$ (bottom horizontal scale). In this figure the horizontal scale has been chosen to be linear in the relative lattice compression $-\Delta a/a_0$. We used the Murnaghan's equation of state to relate the measured pressure to the corresponding change in the lattice constant,[17]

$$\frac{a}{a_0}=\left[\frac{B_0'}{B_0}p+1\right]^{-1/3B_0'}, \tag{1}$$

where p represents the pressure, $a_0=4.36$ Å the lattice constant at room temperature,[15] B_0 the bulk modulus, and B_0' its derivative with respect to p. In the evaluations of Eq. (1) we set $B_0=321.9$ GPa and $B_0'=3.43$. These values correspond to the average of the values of B_0 quoted by Kittel[18] for Si and C, and of the B_0' of Si and C as reported by Mitra *et al.*[13] The value we have taken for B_0 agrees within 15% with the values one can calculate from the measured elastic constant of different SiC polytypes[15] and within 25% with a value obtained from the theoretically calculated elastic constants of 3*C*-SiC.[19] To our knowledge there are no reports in the literature of measurements of B_0' for SiC. When plotted in a scale linear in $\Delta a/a_0$ as in Fig. 2 the measured LO(Γ) and TO(Γ) phonon energies can be described within the experimental error with the following least-squares fits:

$$\begin{aligned}\omega_{\mathrm{TO}}&=(796.5\pm0.3)+(3734\pm30)\left[-\frac{\Delta a}{a_0}\right],\\ \omega_{\mathrm{LO}}&=(973\pm0.3)+(4532\pm30)\left[-\frac{\Delta a}{a_0}\right],\end{aligned} \tag{2}$$

with ω_{TO} and ω_{LO} given in cm^{-1}. The solid lines drawn through the experimental points of Fig. 2 represent the evaluations of Eq. (2).

If we plot the measured LO and TO energies against a linear pressure scale a sublinear dependence of these energies with increasing pressure is obtained. The nonlinearity is related to the nonlinear relationship between Δa and p given by Eq. (1). Quadratic fits to the data give the following results for the pressure dependence.

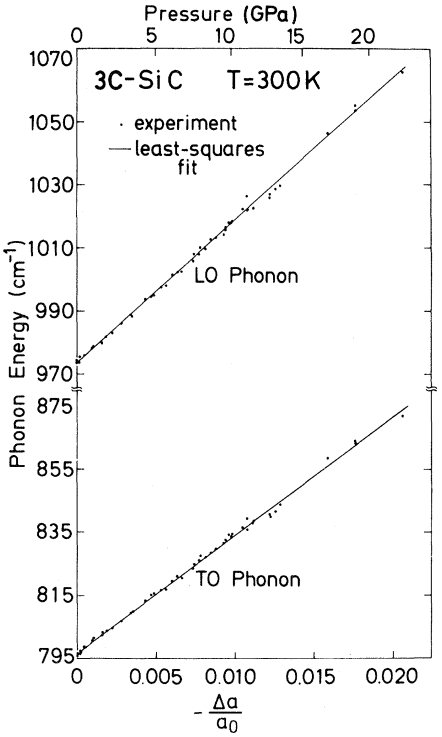

FIG. 2. Dependence of the LO(Γ) and TO(Γ) phonon energies on relative lattice compression (linear lower scale) and pressure (upper scale). The solid lines are least-squares fits to the experimental points with Eq. (2).

$$\begin{aligned}\omega_{\mathrm{TO}}&=(796.2\pm0.3)+(3.88\pm0.08)p\\ &\quad-(2.2\pm0.4)\times10^{-2}p^2,\\ \omega_{\mathrm{LO}}&=(972.7\pm0.3)+(4.75\pm0.09)p\\ &\quad-(2.5\pm0.4)\times10^{-2}p^2,\end{aligned} \tag{3}$$

with ω_{TO} and ω_{LO} in cm^{-1} and p in GPa.

The mode-Grüneisen parameters $\gamma_i=-\partial\ln\omega_i/\partial\ln V$ for the TO(Γ) and LO(Γ) phonons can be obtained from the coefficient of the linear term in $\Delta a/a_0$ of Eq. (2). The values for γ_i are $\gamma_{\mathrm{TO}}=1.56\pm0.01$ and $\gamma_{\mathrm{LO}}=1.55\pm0.01$.

From Figs. 1 and 2 one can see that the LO(Γ)-TO(Γ) splitting increases with increasing pressure. A linear dependence of this splitting on lattice compression is obtained as shown in Fig. 3. When plotted on a linear pressure scale the LO(Γ)-TO(Γ) splitting displays a sublinear behavior. The results of the linear (in $\Delta a/a_0$) and quadratic (in p) least-squares fits are:

$$\begin{aligned}\omega_{\mathrm{LO}}-\omega_{\mathrm{TO}}&=(176.5\pm0.6)+(806\pm50)\left[-\frac{\Delta a}{a_0}\right]\\ &=(176.3\pm0.6)+(8.5\pm0.2)\times10^{-1}p-(2.5\pm1)\times10^{-3}p^2,\end{aligned} \tag{4}$$

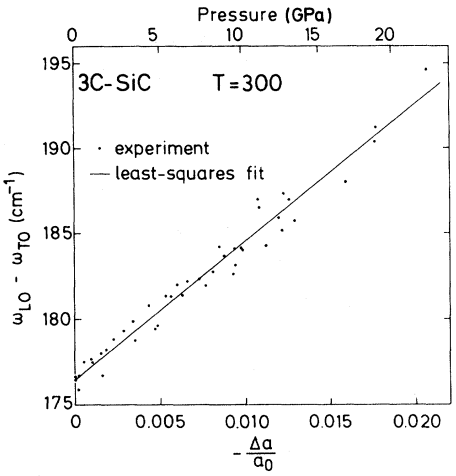

FIG. 3. Dependence of the LO(Γ)-TO(Γ) splitting on lattice compression and pressure. The splitting increases with increasing pressure. The solid line through the experimental points represents a least-squares fit with Eq. (4).

with ω's in cm^{-1} and p in GPa. From Eq. (4) a value of $\gamma_{\text{LO-TO}}=1.52\pm0.05$ is determined. The values of the mode-Grüneisen parameters γ_i reported in this section for the long-wavelength optical phonons of 3*C*-SiC are summarized and tabulated in Table I. Those of Si and C are also displayed in Table I for comparison.

The general behavior of the optical phonons of 3*C*-SiC at Γ agrees with that of other zinc-blende-type materials, in the sense that the optical phonon energies at Γ increase upon compression. The weighted value $d\bar{\omega}/dp=\frac{1}{3}(2d\omega_{\text{TO}}/dp+d\omega_{\text{LO}}/dp)$ from Eq. (3) in the case of 3*C*-SiC is 4.2 cm^{-1}/GPa. This value is almost the same as the mean value $\frac{1}{2}(d\omega_{\text{Si}}/dp+d\omega_C/dp)\simeq4.4$ cm^{-1}/GPa for the optical phonons of Si and C (from Refs. 2 and 6, respectively).

In the case of the mode-Grüneisen parameter the weighted value $\bar{\gamma}=\frac{1}{3}(2\gamma_{\text{TO}}+\gamma_{\text{LO}})\simeq1.55$ for β-SiC is 40% larger than the mean value between Si and C (see Table I). We cannot ascribe at the present a physical meaning to this difference. Very few microscopic calculations of the lattice properties in which γ is not used as an adjustable parameter are found in the literature. Recently, a value of $\gamma=1.8$ has been microscopically calculated for the optical phonons at Γ of Si.[20] In another investigation of the volume dependence of γ a change from ~1 to ~1.4 was calculated by Soma *et al.* for Si when $-\Delta a/a_0$ increases from 0 to ~0.3.[21] By comparing these calculated values of γ for Si and the weighted one for 3*C*-SiC one can conclude that the order of magnitude of $\bar{\gamma}$ is well understood from a theoretical point of view.

The major difference in the qualitative behavior of the optical phonons of 3*C*-SiC upon compression in comparison with other zinc-blende-type semiconductors lies in the pressure dependence of the LO(Γ)-TO(Γ) splitting. For all of the material investgated so far, the splitting decreases with increasing pressure and corresponding the $\gamma_{\text{LO-TO}}$'s are negative (generally at the order of ~-0.5).[2,4,7,8] Our results for $\gamma_{\text{LO-TO}}$ of 3*C*-SiC give a *positive* $\gamma_{\text{LO-TO}}$ with a rather large absolute value (see Table I). The behavior of the LO(Γ)-TO(Γ) splitting is related with the transverse effective charge e_T^*, which is discussed in the next section. Our measurements have definitely confirmed the rather uncertain increase of the LO-TO splitting found by Mitra *et al.*[13] for 3*C*-SiC at very low pressures. We note that in that work the pressure coefficient of the LO-TO splitting changed sign at ~0.4 GPa, a rather unlikely fact which is disproved in our measurements.

TABLE I. Mode-Grüneisen parameters of the long-wavelength optical phonons of 3*C*-SiC, Si, and C.

Material	γ_{TO}	γ_{LO}	$\gamma_{\text{LO-TO}}$
3*C*-SiC[a]	1.56±0.01	1.55±0.01	1.52±0.05
Si[b]	0.98±0.06	0.98±0.06	0
C[c]	1.19±0.09	1.19±0.09	0

[a]Our measurements (see Sec. III).
[b]Reference 2.
[c]Reference 6.

IV. TRANSVERSE EFFECTIVE CHARGE e_T^*

A. 3C-SiC

There is no unique way to assign the electronic charge in a semiconductor to each one of the atoms in the unit cell. However, there is a unique dipole moment induced when an atom is slightly displaced. This dipole moment per unit displacement defines an experimentally measurable effective atomic charge. Specifically, the Born's transverse effective charge $e_T^*(\alpha)$ (the dynamical charge) with α=Si or C, is defined as the macroscopic dipole moment per unit displacement of the sublattice α when the macroscopic electric field in the crystal is kept zero. The charges $e_T^*(\alpha)$ obey the charge neutrality condition[12]

$$e_T^*(\mathrm{Si}) = -e_T^*(\mathrm{C}) \ . \tag{5}$$

For diamond-type crystals, the inversion symmetry additionally requires the effective charges to be equal for the two sublattices which implies that they are zero. In a zinc-blende semiconductor like SiC, however, e_T^* and the corresponding macroscopic dipole polarization are not zero and give rise to the splitting of the long-wavelength LO- and TO-phonon modes,[12]

$$\omega_{\mathrm{LO}}^2(\Gamma) - \omega_{\mathrm{TO}}^2(\Gamma) = \frac{16\pi e_T^{*2}}{\epsilon_\infty a^3 M_{\mathrm{red}}} \ , \tag{6}$$

with $e_T^* = e_T^*(\mathrm{Si}) = -e_T^*(\mathrm{C})$. In Eq. (6), M_{red} is the reduced mass of Si and C, a is the lattice constant, and $\epsilon_\infty = 6.52$[15] denotes the optical (electronic) dielectric constant. Equation (6) implies that e_T^* is proportional to the width of the Reststrahlen band. By measuring with first-order Raman scattering, the shifts of the TO and LO phonons as a function of pressure, the dependence of e_T^* upon compression can be evaluated with Eq. (6). In doing so we encounter the difficulty that the volume dependence of ϵ_∞ is not known experimentally. However, data do exist for Si (Ref. 22) and C (Ref. 23). For both $d\ln\epsilon_\infty / d\ln a \simeq 1.8$. We have taken the same coefficient to evaluate the dependence of ϵ_∞ of 3C-SiC upon compression. With the relationship between a and p given by Eq. (1), the assumed dependence of ϵ_∞ on a, and the data of Figs. (2) and (3), we obtain with Eq. (6) the dependence of e_T^* on pressure (upper scale) or on lattice compression (lower scale) displayed in Fig. 4. Like the LO(Γ)-TO(Γ) splitting e_T^* increases with increasing pressure, which implies an effective transfer of charge from the cation Si to the anion C. This fact may be interpreted by saying that 3C-SiC becomes more *ionic* upon compression.

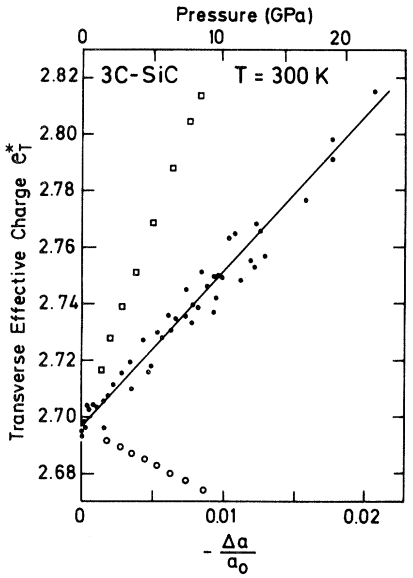

FIG. 4. Dependence on lattice compression and pressure of the transverse effective charge. The full points were obtained from the measured pressure dependence of the LO and TO phonons of Figs. 2 and 3. The solid line represents a least-squares fit with Eq. (7). The square are the results of the full pseudopotential calculations [Eq. (15)]. The open circles are the predictions of the bond-orbital model [Eq. (10]. In both cases the calculated transverse effective charges for $\Delta a = 0$ were renormalized to the experimental value.

The experimental points of Fig. 4 can be fitted with the linear expression:

$$e_T^* = (2.697 \pm 0.004) - (5.45 \pm 0.10)\frac{\Delta a}{a_0} \ . \tag{7}$$

The fit is given by the solid line in the figure. From Eq. (7) a value of $\gamma_{e_T^*} = -\partial\ln(e_T^*)/\partial\ln V = 0.67$ is obtained.

Two different types of approaches have been used to calculate e_T^* and its volume dependence. One approach is based on semiempirical models of the tetrahedral bond while the other one involves a microscopic formulation in terms of the linear response function of the crystal to an external electric field. This function can be calculated with pseudopotential theory. Within the semiempirical models, the bond-orbital model of Harrison is perhaps the more elaborate one.[12] This model gives (pp. 218–224 of Ref. 12)

$$e_T^* = -\Delta Z + \frac{20}{3}\alpha_p - \tfrac{8}{3}\alpha_p^3 \ , \tag{8}$$

where ΔZ is one-half the difference in core charges between the anion and the cation ($\Delta Z=0$ for SiC), and α_p is the polarity or ionicity of the bond as defined in Ref. 12: for 3C-SiC $\alpha_p=0.26$. The dependence of the polarity on lattice compression is given by [see Eqs. (9)–(23) in Ref. 12]

$$\frac{\partial\alpha_p}{\partial(\Delta a/a_0)}=2\alpha_p(1-\alpha_p^2)\ . \tag{9}$$

With Eqs. (8) and (9) we obtain the following dependence of the transverse effective charge:

$$e_T^*=1.69+2.97\frac{\Delta a}{a_0}\ . \tag{10}$$

Within this model e_T^* diminishes with increasing pressure contrary to the experimental observations of Fig. 4. The predictions of Eq. (10) are represented in this figure by the open circles, where the charge calculated for $\Delta a=0$ was renormalized to the experimental value. The failure of the bond-orbital model to describe the pressure dependence of e_T^* may arise in having completely neglected the dependence upon compression of the ionic contribution to the effective gap which enters in the definition of α_p. This represents a good approximation for the III-V and the II-VI compounds. It is doubtful, however, to what extent it is justifiable for 3C-SiC (and other possible IV–IV bonds) a material for which the ionicity has a completely different character than in the III-V and II-VI compounds. We should add, however, that Eqs. (8) and (9) predict a positive $\gamma_{e_T^*}$ for $\alpha_p>0.9$, an ionicity much larger than that of SiC.

We present now a calculation of e_T^* for 3C-SiC and its pressure dependence based on the microscopic pseudopotential expression for e_T^* [see Eq. (4.6) of Ref. 11 and Appendix A of Ref. 4]:

$$e_T^*=\frac{2}{N}\sum_{\vec{G}\neq 0}\sum_{nn'\vec{k}}\frac{\theta_{n\vec{k}}(1-\theta_{n'\vec{k}})}{(E_{n\vec{k}}-E_{n'\vec{k}})^2}\langle n\vec{k}\,|\,p_x\,|\,n'\vec{k}\rangle\langle n'\vec{k}\,|\,e^{i\vec{G}\cdot\vec{\tau}}\,|\,n\vec{k}\rangle$$
$$\times G_x[iv_s(G)\sin\vec{G}\cdot\vec{\tau}-v_a(G)\cos\vec{G}\cdot\vec{\tau}]\ . \tag{11}$$

The Bloch states $|nk\rangle$ and the energies $E_{n\vec{k}}$ of the electrons are obtained in the framework of the local empirical pseudopotential method.[24] In Eq. (11), N denotes the number of unit cells, the $\vec{G}$'s are the reciprocal-lattice vectors, and $\vec{p}$ is the linear momentum operator. Furthermore, $\theta_{n\vec{k}}=1$ if n is one of the four valence bands and $\theta_{n\vec{k}}=0$ otherwise. The crystal potential, which enters Eq. (11) explicitly as well as implicitly via the Bloch states, is in a plane wave basis $\langle\vec{k}+\vec{G}|v|\vec{k}+\vec{G}'\rangle=v(\vec{G}-\vec{G}')$ with

$$v(\vec{G})=v_s(G)\cos\vec{G}\cdot\vec{\tau}+iv_a(G)\sin\vec{G}\cdot\vec{\tau}\ . \tag{12}$$

Here $\vec{\tau}=(a/8)(1,1,1)$ and

$$v_s(G)=\tfrac{1}{2}[v_{\mathrm{Si}}(G)+v_{\mathrm{C}}(G)]\ ,$$
$$v_a(G)=\tfrac{1}{2}[v_{\mathrm{Si}}(G)-v_{\mathrm{C}}(G)]\ , \tag{13}$$

are the symmetric and antisymmetric pseudopotential form factors expressed in terms of the atomic form factors. For zero pressure, we used the empirical form factors of Ref. 24 for Si and those of Ref. 25 for C, which adequately reproduce the band structure of Si and diamond, respectively. To calculate e_T^* and its pressure dependence, the atomic form factors $v(q)$ are needed at different q values than in Si and C. In accordance with empirical pseudopotential theory,[24] we first extrapolated the empirical Si form factors $v_{\mathrm{Si}}(q)$ by setting $v_{\mathrm{Si}}(0)=-\frac{2}{3}E_F=-0.613$ Ry and truncating $v_{\mathrm{Si}}(q)$ beyond $q_{\mathrm{cut}}=3k_F=2.8$ a.u. and then interpolated them by a cubic spline.

For C, where a local pseudopotential model is a rather crude approximation, $v_{\mathrm{C}}(0)=-1$ Ry and $q_{\mathrm{cut}}=3.32$ a.u. were considered as fitting parameters to reproduce the known band structure of 3C-SiC, in the manner discussed in Ref. 26. The resulting form factors have been normalized to the unit cell volume of 3C-SiC and are given in Table II. For the band calculation 89 plane waves were included and 10 special $\vec{k}$ points[27] to perform the $\vec{k}$ summation in Eq. (11). This calculation gives $e_T^*=2.81$. The effect of the pressure on e_T^* arises

TABLE II. Pseudopotential form factors (in Ry) for 3C-SiC used to calculate e_T^* with Eq. (11). The derivatives with respect to the reciprocal-lattice vectors needed to evaluate Eq. (18) and Eqs. (A7) and (A8) from Ref. 4 are listed.

G^2	v_{Si}	v_C	v_s	v_a	$\frac{dv_{Si}}{dG}$	$\frac{dv_C}{dG}$
3	$-0.218^{(a)}$ $-0.19^{(b)}$	$-0.460^{(a)}$ $-0.55^{(b)}$	$-0.339^{(a)}$	$0.121^{(a)}$	$0.749^{(a)}$ $0.72^{(b)}$	$0.230^{(a)}$ $0.60^{(b)}$
4	$-0.063^{(a)}$	$-0.409^{(a)}$	$-0.236^{(a)}$	$0.173^{(a)}$		
8	$0.172^{(a)}$ $0.15^{(b)}$	$-0.126^{(a)}$ $-0.03^{(b)}$	$0.023^{(a)}$	$0.149^{(a)}$	$\simeq 0^{(a)}$	$0.521^{(a)}$
11	$0.110^{(a)}$	$0.129^{(a)}$	$0.120^{(a)}$	$-0.009^{(a)}$		
12	$0.068^{(a)}$	$0.188^{(a)}$	$0.128^{(a)}$	$-0.060^{(a)}$		
16	$0^{(a)}$	$0.088^{(a)}$	$0.044^{(a)}$	$-0.044^{(a)}$		

[a]From Ref. 26, used for the complete numerical and the approximate analytical calculation.
[b]From Refs. 22, 29, and 30, used for analytical calculation only.

from the change in the lattice constant. This affects the pseudopotential form factors in two ways: (i) the form factors $v_{S,A}(q)$ are needed at the pressure-shifted reciprocal-lattice vectors and (ii) they have to be renormalized. The atomic form factors v_{Si},v_C are screened ionic pseudopotentials, e.g.,

$$v_{\mathrm{Si,cryst}}(\vec{q})=\frac{1}{\Omega_0\epsilon(\vec{q})}\int d^3r\, v_{\mathrm{Si,ion}}(r)e^{-i\vec{q}\cdot\vec{r}}\,, \quad (14)$$

and depend on the lattice constant via the atomic volume $\Omega_0=a^3/8$. The dielectric function $\epsilon(\vec{q})$ is insensitive to small changes in $\vec{q}$ for the momenta $\vec{q}\gtrsim(2\pi/a)\sqrt{3}$ which enter the band calculation. As customary, we have neglected this small effect. In addition, we adopt the rigid-ion approximation where $v_{\mathrm{Si,ion}}(\vec{q})$ does not depend on the lattice constant.

The results of the full pseudopotential calculation are represented by

$$e_T^*=2.81-14.1\frac{\Delta a}{a_0}\,. \quad (15)$$

The squares of Fig. 4 were evaluated with Eq. (15), with the calculated effective charge e_T^* renormalized for $\Delta a=0$ to the experimental value (2.697). The principal prediction of the pseudopotential model is that the transverse effective charge increases with pressure in 3C-SiC, a fact which agrees with the experimental observation. This is in contrast to the behavior of e_T^* in the III-V and II-VI semiconductors where the model gives a decreasing e_T^* with decreasing nearest-neighbor distance, also in accord with experiment.[4] The lack of quantitative agreement between the experimental and the calculated magnitude of the change in e_T^* with Δa_0 is to be attributed, at least in part, to uncertainties in the pseudopotential form factors. Similar discrepancies have been found for the III-V compounds.[4]

Equation (11) can be simplified by using a model similar to that of Heine and Jones.[11,4,28] This simplification leads to some physical insight into expersion (11) and to the possibility of calculating e_T^* with an analytic expression. Neglecting all pseudopotential form factors with $G>(2\pi/a)\sqrt{3}$ one gets for the e_T^* of 3C-SiC:[11]

$$e_T^*=-8\frac{v_s(3)v_a(3)}{v_s^2(3)+v_a^2(3)}=-4\frac{v_{\mathrm{Si}}^2(3)-v_{\mathrm{C}}^2(3)}{v_{\mathrm{Si}}^2(3)+v_{\mathrm{C}}^2(3)}\,. \quad (16)$$

This expression can be differentiated with respect to the relative lattice compression by using the following equation for the derivatives of the form factors[22]:

$$\frac{dv(G)}{da}=-\frac{3}{a}\left[v(G)+\tfrac{1}{3}G\frac{dv(G)}{dG}\right]. \quad (17)$$

The derivatives $dv(G)/dG$ can be evaluated from the slope of the interpolation curves which give v as a function of G, as displayed in Fig. 5. From Eq. (16) and the prescriptions of Eq. (17) one obtains:

$$\frac{\partial e_T^*}{\partial\left[\frac{\Delta a}{a_0}\right]}=16\frac{v_{\mathrm{Si}}(3)v_{\mathrm{C}}(3)}{[v_{\mathrm{Si}}^2(3)+v_{\mathrm{C}}^2(3)]^2}\times G\left[v_{\mathrm{Si}}(3)\frac{dv_{\mathrm{C}}(3)}{dG}+v_{\mathrm{C}}(3)\frac{dv_{\mathrm{Si}}(3)}{dG}\right]. \quad (18)$$

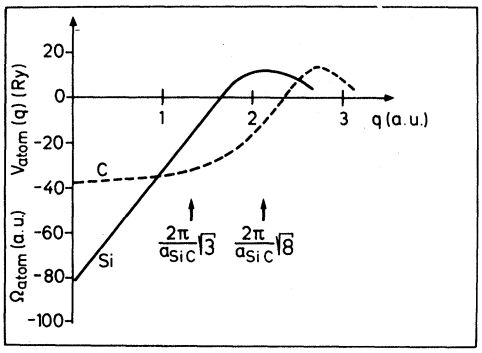

FIG. 5. Local empirical atomic pseudopotential form factors for Si and C as a function of the wave vector q. The form factors have been scaled to the same atomic volume (that of 3C-SiC). The first reciprocal-lattice vectors of 3C-SiC are marked by arrows.

With the values tabulated in Table II for $G=(2\pi/a)\sqrt{3}$, the following dependence for e_T^* is calculated from Eqs. (16) and (18),

$$e_T^*=2.5-9.2\frac{\Delta a}{a_0}\ , \tag{19}$$

in quite reasonable agreement with the experiment (Eq. 7) especially when considering the approximations involved.

One can see in Eq. (18) that the sign of $\partial e_T^*/[\partial(\Delta a/a_0)]$ is given by the sign of the expression in brackets, as the $v_i(3)$'s are negative for both Si and C. This expression has a negative sign in 3C-SiC due to the fact that $dv_C(3)/dG$ is very small [a factor 3.3 smaller than $dv_{Si}(3)/dG$ is shown in Table II]. That fact is a rather crucial point: For the III-V and II-VI compounds

$$\frac{dv_{\text{anion}}(3)}{dG}>\frac{dv_{\text{cation}}(3)}{dG}$$

and consequently it turns out that $\partial e^*/[\partial(\Delta a/a_0)]>0$. This weak dependence of v_3(C) on q for $q\simeq G=(2\pi/a)\sqrt{3}$ presumably arises from the very small core radius of C.[24] As SiC is compressed a transfer of electronic charge takes place from the Si atoms to the C atoms [e_T^* increases, see Eq. (5)] in order to take advantage of the strong attractive potential associated with the small core radius of C. In the language of pseudopotential theory $v_a(3)$ increases with increasing q (decreasing lattice constant), as displayed in Fig. 5. The increase of $v_a(3)$ represents an attraction of the valence electrons towards the C sites.

Equation (16) includes only the contribution to e_T^* of the pseudopotential components $v(3)$. A modified expression of this equation can be obtained by keeping in Eq. (11) not only the $v(3)$'s but also the $v(8)$ components of the pseudopotentials [see Eqs. (A7) and (A8) of Ref. 4]. With those expressions we obtained almost the same results for the derivatives of the effective charge with respect to a as given by Eq. (18). As it is easier to obtain a physical insight into the microscopic processes which produce the increase of e_T^* with pressure in 3C-SiC we preferred to use for the discussion the simplest possible expressions for e_T^*, i.e., Eqs. (16) and (18).

At this point we should mention that the set of pseudopotential form factors used for the calculation of e_T^* [and listed under (a) in Table II] is probably not unique. While they were adjusted to fit a few experimental data for 3C-SiC, it is also possible to perform the calculation with the form factors of elemental Si and C properly interpolated on renormalized so as to correct for changes in reciprocal-lattice vectors, changes in atomic volumes, and changes in the screening by the valence electrons. In this manner we obtained from Refs. 29 and 30 the pseudopotential form factors listed under (b) in Table II. With these form factors we repeated the analytical evaluation of Eqs. (16) and (18) and obtain

$$\begin{aligned} &e_T^*=3.15\ , \\ &\frac{\partial e_T^*}{\partial(\Delta a/a_0)}=-5.43\ , \end{aligned} \tag{20}$$

in excellent agreement with experiment. Table III summarizes the experimental and the calculated values of e_T^* and of the "Grüneisen parameters" of e_T^*.

We attempt now to give a plausible, though heuristic, simple interpretation of the striking fact that in the III-V and II-VI compounds e_T^* and α_p increase with increasing a while in SiC they decrease. The features of the dependence of the polarity α_p on lattice constant can be obtained as follows. For $a=0$ and for $a=\infty$, $\alpha_p=0$: In the former case both atoms share all electrons while in the latter the atoms are neutral. This α_p as a function of a must have a maximum at a lattice constant a_M (note that the argument is similar to that followed to derived "Laffer's curve" in taxation theory). Depending on whether the equilibrium lattice constant a_0 is smaller or larger than a_M, one finds an increase or a decrease of α_p (and thus of e_T^*) with increasing lattice constant, respectively. The former case seems to apply to the III-V's and

TABLE III. Mode-Grüneisen parameters of the transverse effective charge of 3C-SiC and transverse effective charge e_T^* as measured experimentally and as calculated with various pseudopotential approaches.

	Experiment [Eq. (7)]	Full pseudotential calculation [Eq. (15)]	Simplified pseudopotential calculation [Eq. (19)] [form factors (a) of Table II]	Simplified pseudopotential calculation [Eq. (20)] [form factors (b) of Table II]	Bond-orbital model [Eq. (10)]
$\gamma_{e_T^*}$	0.67	1.67	1.23	0.58	−0.59
e_T^*	2.70	2.81	2.5	3.15	1.69

II-VI's, the latter to 3C-SiC, probably because of the large difference in the atomic radii of Si and C.

B. Other IV−IV tetrahedral bonds

In view of the success reached above with our theoretical estimates of the effective charge of 3C-SiC and its pressure derivative, we shall now, as a by-product, evaluate the effective charges of other fictitious ordered IV-IV zinc-blende-type compounds. The results, while mainly of academic interest, may be applicable to calculate the effective charge of IV−IV bonds, and, by analogy of local modes of isoelectronic impurities in Ge or Si (e.g., Si in Ge or C in Si).

The simplest way of estimating e_T^* is no doubt the bond-orbital model of Harrison [Eq. (8)]. We have already shown, however, that this method is somewhat suspect in the case of IV−IV bonds (see Table III). We shall use it, nevertheless, for the sake of comparison with the more reliable pseudopotential results.

In order to evaluate Eq. (8) we must obtain a value for the polarity α_p. This can be done in the manner proposed by Harrison,[12]

$$\alpha_p = \frac{V_3}{(V_2^2+V_3^2)^{1/2}}\,,$$
$$V_3 = \tfrac{1}{2}(E_p^{\text{cation}} - E_p^{\text{anion}})\,, \tag{21}$$
$$V_2 = 2.16(\hbar^2/md^2)\,,$$

where E_p are the atomic one-electron energies of the p valence electrons, which we obtain from Ref. 31, and d the nearest-neighbor distance. With Eqs. (21) we calculate the values of α_p listed in Table IV. The values of d were obtained by averaging those of the pure elemental constituents.

A recent paper by Shen and Cardona reports the infrared absorption spectrum produced by Si "impurities" in a $Ge_{0.9}Si_{0.1}$ crystalline alloy.[32] From these data we evaluate a total charge for the Si−Ge bond $e_T^*=0.10$ in reasonable agreement with the estimates of Table IV, especially with the bond charge model calculation. The infrared spec-

TABLE IV. Nearest neighbor distances d, static charges Z^*, polarity α_p, and dynamic charges e_T^* obtained with the bond-orbital model and with the pseudopotential method. In the formula of the compound (e.g., SiC) the most *electropositive* element (Si) is given first. The charges given thus are positive for this element.

	d (Å)	Z^{*a}	$\alpha_p{}^a$	e_T^{*a}	e_T^{*b}	e_T^{*c}
SiC	2.53	1.02	0.26	1.7	2.53	2.8
GeC	2.00	1.02	0.3	1.94	1.43	1.2
SnC	2.18	1.60	0.4	2.50	1.94	metallic
SiGe	2.40	0.11	0.03	0.19	0.57	0.6
SnSi	2.58	0.47	0.12	0.77	0.20	0
SnGe	2.63	0.35	0.09	0.53	0.66	0.5

[a]Bond-orbital model [Eqs. (8) and (21)] and Ref. 12.
[b]Pseudopotential calculation [Eq. (16)].
[c]Complete numerical calculation [Eq. (11)].

trum of the $Ge_{0.9}$-$Si_{0.1}$ alloy contains various distinct features, among them a local mode (ω_L) at 400 cm^{-1}, a quasilocal mode at 110 cm^{-1} (ω_{QL}), and a broad continuum corresponding to the fundamental absorption of Ge. The dynamical charge evaluated for each one of these modes is $e_T^*(\omega_L)=0.07$, $e_T^*(\omega_{QL})=0.31$, e_T^* (continuum)$=0.17$. The values of $e_T^*=0.10$ given above represent the weighted average of these values.

V. CONCLUSIONS

We have measured the hydrostatic pressure dependence of the long-wavelength optical phonons of 3*C*-SiC. We obtained for the mode-Grüneisen parameters of the LO and TO phonons $\gamma_{LO}=1.55\pm0.01$ and $\gamma_{LO}=1.56\pm0.01$, respectively. These values are somehow larger than those for the optical phonons of Si and C.

Contrary to the case of the III-V and II-VI semiconductors, the LO(Γ)-TO(Γ) splitting of 3*C*-SiC increases with increasing pressure. The corresponding mode-Grüneisen parameter is $\gamma_{LO\text{-}TO}=1.52\pm0.05$, which does not fit into the systematics of the III-V and II-VI compounds. The increase of the LO(Γ)-TO(Γ) splitting implies an increase of the transverse effective charge upon compression. We have shown that the dependence of e_T^* on lattice compression can be explained with a microscopic formulation of e_T^*, in terms of pseudopotentials. Semiempirical models, such as the bond-orbital model, are unable to explain the behavior of e_T^* under pressure in 3*C*-SiC.

We thus conclude that the pressure dependence of e_T^* is a sensitive probe of the electronic structure as well as a stringent test for theoretical calculations of e_T^*. As a by-product we have calculated the dynamical charges of all possible fictitious IV-IV semicondutors. In the case of Ge-Si we have compared the results with experimental data for the infrared absorption in $Ge_{0.9}Si_{0.1}$.

ACKNOWLEDGMENTS

It is a pleasure to thank Dr. W. J. Choyke for the samples of 3*C*-SiC. The help of Mr. W. Dieterich in loading the diamond cell is gratefully acknowledged. One of us (P.V.) wants to acknowledge the "Fonds für die Förderung der wissenschaftlichen Forschung in Österreich," Projekt Nr. 4236.

[1]J. D. Barnett, S. Block, and G. J. Piermarini, Rev. Sci. Instrum. 44, 1 (1973); G. J. Piermarini, S. Block, J. D. Barnett, and R. A. Forman, J. Appl. Phys. 46, 2774 (1975).

[2]B. A. Weinstein and G. J. Piermarini, Phys. Rev. B 12, 1172 (1975).

[3]B. Welber, M. Cardona, C. K. Kim, and S. Rodriguez, Phys. Rev. B 12, 5729 (1975).

[4]R. Trommer, H. Müller, M. Cardona, and P. Vogl, Phys. Rev. B 21, 4869 (1980).

[5]D. Olego, M. Cardona, and H. Müller, Phys. Rev. B 22, 894 (1980).

[6]B. J. Parsons, Proc. R. Soc. London Ser. A 352, 397 (1977).

[7]R. Trommer, E. Anastassakis, and M. Cardona, in *Light Scattering in Solids,* edited by M. Balkanski, R. C. C. Leite, and S. P. S. Porto (Flammarion, Paris, 1976), p. 396; R. Trommer, Ph.D. thesis, University of Stuttgart, 1977 (unpublished).

[8]B. A. Weinstein, Solid State Commun. 24, 595 (1977).

[9]C. Carlone, D. Olego, A. Jayaraman, and M. Cardona, Phys. Rev. B 22, 3877 (1980).

[10]S. C. Yu, I. L. Spain, and E. F. Skelton, Solid State Commun. 25, 49 (1978),

[11]P. Vogl, J. Phys. C 11, 251 (1978).

[12]W. Harrison, in *Electronic Structure and Properties of Solids* (Freeman, San Francisco, 1980).

[13]S. S. Mitra, O. Brafman, W. B. Daniels, and R. K. Crawford, Phys. Rev. 186, 942 (1969).

[14]K. Syassen and W. Holzapfel, Phys. Rev. B 18, 5826 (1978).

[15]See, for example, Appendix II of *Silicon Carbide 1973,* edited by R. C. Marshall, J. W. Faust, and C. E. Ryan (University of South Carolina Press, Columbia, 1974), and references therein.

[16]D. W. Feldman, J. H. Parker, W. J. Choyke, and L. Patrick, Phys. Rev. 173, 787 (1968).

[17]F. D. Murnaghan, Proc. Natl. Acad. Sci. U.S.A. 30, 244 (1944).

[18]C. Kittel, in *Introduction to Solid State Physics,* 5th edition (Wiley, New York, 1976).

[19]K. B. Tolpygo, Fiz. Tverd. Tela 2, 2655 (1960) [Sov. Phys.—Solid State 2, 2367 (1960)].

[20]H. Wendel and R. Martin, Phys. Rev. B 19, 5251 (1979).

[21]T. Soma, Y. Saitoh, and H. Matsuo, Solid State Commun. 39, 913 (1981).

[22]M. Cardona, in *Atomic Structure and Properties of*

Solids, edited by E. Burstein (Academic, New York, 1972), p. 514.
[23]J. A. van Vechten, Phys. Rev. 182, 891 (1969).
[24]M. L. Cohen and V. Heine, in *Solid State Physics,* edited by H. Ehrenreich, F. Seitz, and D. Turnbull (Academic, New York, 1970), Vol. 24, p. 37.
[25]W. van Haeringen and H. G. Junginger, Solid State Commun. 7, 1135 (1969).
[26]H. G. Junginger and W. van Haeringen, Phys. Status. Solidi 37, 709 (1970).
[27]H. J. Monkhorst and J. D. Pack, Phys. Rev. B 13, 5188 (1976).
[28]V. Heine and R. Jones, J. Phys. C 2, 719 (1969).
[29]M. L. Cohen and T. K. Bergstresser, Phys. Rev. 141, 789 (1966).
[30]W. Saslow, T. K. Bergstresser, and M. L. Cohen, Phys. Rev. Lett. 16, 354 (1966).
[31]F. Herman and S. Skillman, in *Atomic Structure Calculations* (Prentice Hall, Englewood Cliffs, 1963).
[32]S. C. Shen and M. Cardona, Solid State Commun. 36, 327 (1980).